Forschung Wissenschaft

ENDOR of Organic Radicals in Solution*

By KLAUS MÖBIUS and KLAUS-PETER DINSE
II. Physikalisches Institut der Freien Universität Berlin, Berlin 33 (Germany)

Summary

A survey is given over the ENDOR method as applied to organic doublet radicals in solution. After discussing the experimental requirements for successful ENDOR-in-solution work, selected examples are presented which demonstrate the power and limitations of the ENDOR method. The examples chosen cover ENDOR work on protons, ^{19}F, ^{14}N, and ^{13}C nuclei in radicals dissolved in isotropic and anisotropic solutions. Some emphasis is put on ^{14}N-ENDOR in liquid crystals because by this technique quadrupole couplings of radicals in solution can be measured directly from the line positions. In an Appendix a complete survey is given of ENDOR-in-solution publications.

Introduction

Electron-Nuclear-Double-Resonance (ENDOR) has already proven to be a very powerful spectroscopic method for the investigation of the magnetic interactions between an unpaired electron and nuclei in complex paramagnetic systems. In an ENDOR experiment the intensity of an electron spin resonance (EPR) signal is monitored as the frequency of a nuclear spin resonance (NMR) radio source is swept. The main advantage of ENDOR compared with EPR is the better resolution of the spectra obtained, as is demonstrated in Fig. 1.

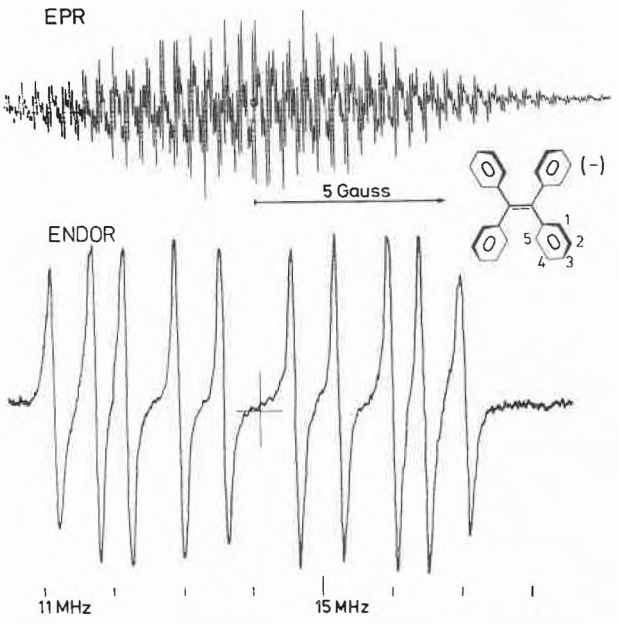

Figure 1. EPR and ENDOR spectra of the tetraphenyl-ethylene radical anion [53]

Although the ENDOR spectrum exhibits much fewer lines, it contains the same information about the hyperfine interactions in this radical as the confusing multiline EPR spectrum.

In this paper we start with a brief description of the ENDOR experiment from which we deduce the experimental requirements for successful ENDOR-in-solution work. In the subsequent section we discuss with some length selected examples which demonstrate the power and limitations of the ENDOR method. This discussion is divided into two main parts: 1. ENDOR in isotropic solutions and 2. ENDOR in liquid crystals.

In an Appendix a complete survey is given of the ENDOR-in-solution results hitherto reported in the literature.

The ENDOR Experiment

The ENDOR experiment will be described with the aid of Fig. 2, showing the energy level scheme of a radical containing 4 equivalent protons in a magnetic field. The interactions responsible for the various splittings are summarized in the following Spin-Hamiltonian:

$$\mathcal{H}/h = \frac{\gamma_e}{2\pi} \boldsymbol{H}_0 \boldsymbol{S} - \frac{\gamma_n}{2\pi} \boldsymbol{H}_0 \boldsymbol{I} + \boldsymbol{A} \cdot \boldsymbol{S}\boldsymbol{I}. \qquad (1)$$

The main splitting is due to the *electronic* ZEEMAN interaction $\frac{\gamma_e}{2\pi} \boldsymbol{H}_0 \boldsymbol{S}$, the interactions responsible for the other splittings are the *nuclear* ZEEMAN and hyperfine interactions $\frac{\gamma_n}{2\pi} \boldsymbol{H}_0 \boldsymbol{I}$ and $\boldsymbol{A} \cdot \boldsymbol{S}\boldsymbol{I}$, respectively. The hfs coupling constant A is scalar as long as radicals in solution are considered. In nematic liquid crystals A contains contributions from the traceless part of the hfs tensor.

In the strong field approximation the energy eigenvalues, classified by the magnetic spin quantum numbers m_s and m_I, are given by

$$E_{m_s m_I}/h = \frac{\gamma_e}{2\pi} H_0 m_s - \frac{\gamma_n}{2\pi} H_0 m_I + A m_s m_I, \qquad (2)$$

i.e. for a specific m_s state the hfs levels are equidistant.

* Presented at the Chemical Colloquium of the University of Zürich (Switzerland) on February 15, 1972 by K. MÖBIUS.

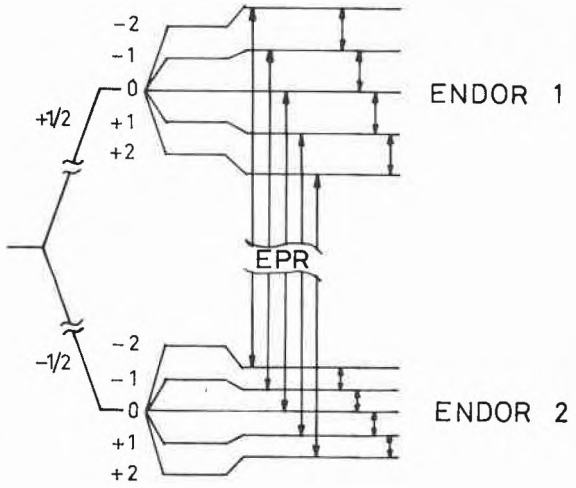

$$E/h = (\gamma_e/2\pi)H_0 m_S - (\gamma_n/2\pi)H_0 m_I + A m_S m_I$$

$$\nu_{ENDOR} = |\nu_n \pm A/2|, \quad \Delta m_S = 0, \quad \Delta m_I = \pm 1$$

$$\nu_n = (\gamma_n/2\pi)H_0$$

Figure 2. Energy level scheme of a radical containing 4 equivalent protons in a magnetic field ($A < 0$)

In an EPR experiment, therefore, by irradiating at a fixed frequency and sweeping the magnetic field one observes 5 EPR lines with binomial intensity distribution. In an ENDOR experiment the sample is irradiated with two rf fields: With the microwave field an EPR transition $\Delta m_s = \pm 1$, $\Delta m_I = 0$ is saturated at a fixed magnetic field. Additionally an rf field of varying frequency is applied saturating the NMR transitions $\Delta m_I = \pm 1$ of the nuclei coupled to the unpaired electron. As a result EPR transitions can be desaturated by the NMR transitions provided both transitions have energy levels in common. In an ENDOR spectrum, therefore, the enhanced EPR signal intensity is plotted versus the NMR frequency, showing that ENDOR is a variant of NMR, the unpaired electron serving as the detector.

Because of the pumping of the microwave transitions and the quantum transformation from NMR to EPR, ENDOR is more sensitive than NMR roughly by a factor of 10^5. Compared with EPR, however, one loses at least a factor of 10. On the other hand, one gains in resolution, because every group of equivalent nuclei—no matter how many nuclei are involved—contributes only 2 ENDOR lines due to the first order degeneracy of the NMR transitions within these groups for a given m_s state. Especially for low symmetry radicals this gain in resolution can be very drastic.

The 2 ENDOR lines are displayed for every nucleus in a doublet radical at the following frequencies:

$$\nu_{ENDOR} = |\nu_n \pm A/2|, \qquad (3)$$

where $\nu_n = \frac{\gamma_n}{2\pi} H_0$ is the nuclear LARMOR frequency. For protons, A is generally smaller than ν_n, so that both ENDOR lines are symmetrically displayed about ν_n and separated by A.

The gain in resolution has to be paid for by additional experimental effort compared with EPR. The reason for the experimental difficulties can be deduced from Fig. 3.

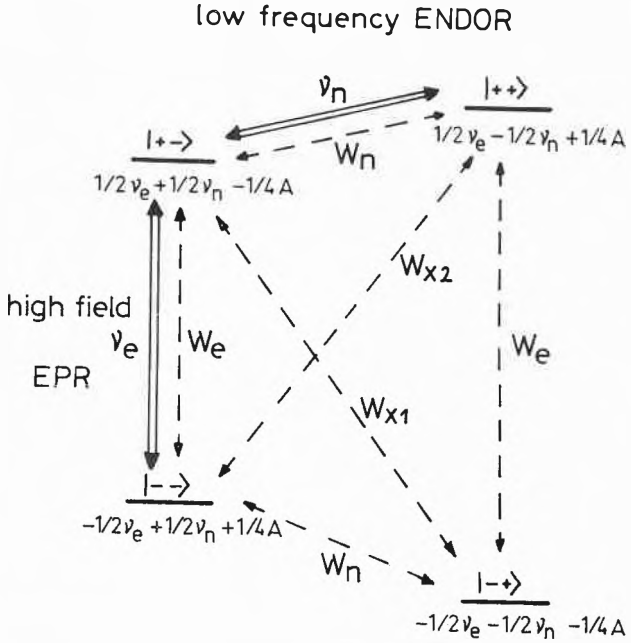

Figure 3. Energy level scheme for $S = 1/2$, $I = 1/2$. For the notation used see text

It shows the energy levels for the most simple case $S = 1/2$, $I = 1/2$, both spins being coupled by an hfs constant $A > 0$, $A/2 > \nu_n$. Two different EPR and two different NMR transitions can be induced, the frequencies being $\nu_e = \frac{\gamma_e}{2\pi} H_0 \pm A/2$, $\nu_n = \left|\frac{\gamma_n}{2\pi} H_0 \pm A/2\right|$, respectively.

The relaxation rates between the energy states are denoted by W_e, W_n, W_{x_1}, and W_{x_2}. For isolated molecules in solution the electronic relaxation W_e is mainly induced by modulation of the anisotropic electron ZEEMAN, the electron nuclear dipole, and the spin rotational interactions. W_n, however, is mainly determined by the pseudo-secular term $I_\pm S_z$ in the anisotropic hfs coupling. Cross relaxations W_{x_1}, W_{x_2} are due to nonsecular terms $I_\pm S_\mp$ and $I_\pm S_\pm$ of the same interaction. For protons in aromatic radicals they can be neglected[3]. In case of ^{14}N and ^{13}C radicals, however, their influence on the ENDOR intensity ratio could be detected (*vide infra*).

In a phenomenological description of the ENDOR effect, the ENDOR enhancement can be explained by a change of the effective electron spin lattice relaxation time T_{1e}. This is equivalent to a solution of modified BLOCH equations. The change in T_{1e} is achieved by

opening an additional relaxation path $|+-\rangle \rightarrow |++\rangle \rightarrow |-+\rangle \rightarrow |--\rangle$ (see Fig. 3). The magnitude of ΔT_{1e}—and therefore the ENDOR enhancement—depends on the rf induced net transition rate between $|+-\rangle$ and $|++\rangle$ and on the relative magnitude of the relaxation rates W_e and W_n.

From Fig. 3 we can deduce the three main conditions which have to be fulfilled for successful ENDOR-in-solution work:

At first one has to saturate one of the EPR transitions, which is equivalent to the condition

$$\gamma_e^2 H_1^2 T_{1e} T_{2e} \approx 1. \tag{4}$$

The same condition holds for the irradiated NMR transition in order to compete effectively with the direct relaxation path:

$$\gamma_n^2 H_2^2 T_{1n} T_{2n} \geqslant 1. \tag{5}$$

As can easily be seen by analogy with an electric circuit diagram in which the relaxation rates are treated as conductances, the optimum ENDOR enhancement is achieved for

$$W_n / W_e = 1, \tag{6}$$

if one neglects any cross relaxation. This third condition has to be approximated by choosing suitable solvents and sample temperatures. Because of the large difference in the transition frequencies ν_n and ν_e, the spectral density functions of the perturbing local fields show a different dependence on the rotational correlation time τ_R. As τ_R can be related to the temperature T and the macroscopic viscosity η of the solvent by the STOKES-EINSTEIN relation, the ratio W_n / W_e is given by[5]

$$\frac{W_n}{W_e} = C \cdot \left(\frac{\eta}{T}\right)^2, \tag{7}$$

C being a constant independent of temperature. As the viscosity depends strongly on T, it is obvious, that optimum ENDOR enhancement requires a carefully selected temperature. Fortunately this requirement can be met for a variety of common solvents, like for instance toluene, dimethoxyethane, isopentane, by spectroscopying just above their melting points.

These three conditions can be summarized to

$$H_2 \geqslant \left(\frac{T_{2e}}{T_{2n}}\right)^{1/2} \cdot \frac{\gamma_e}{\gamma_n} \cdot H_1, \tag{8}$$

which enables one to estimate the magnitude of the required NMR field H_2. For common organic doublet radicals the factor containing the homogeneous EPR and NMR linewidth parameters T_{2e} and T_{2n} is in the range of 0.3 to 1. From the EPR saturation behaviour of these radicals the microwave field H_1 can be estimated to be of the order of 50 mOe (amplitude, rotating frame). It follows that proton ENDOR already requires NMR fields as high as 10 to 30 Oe (amplitude, rotating frame). An rf power of about 500 W is needed to produce radio frequency fields of this magnitude over a reasonable sample volume. This causes problems in rf pick-up and long term stability of the spectrometer. The first successful ENDOR-in-solution work on organic radicals was therefore published not earlier than 1964 by HYDE and MAKI[1], although FEHER[38] has performed first low temperature ENDOR experiments already in 1956.

At helium temperature $T_{2e}/T_{2n} \ll 1$, and furthermore the microwave saturation field H_1 is much smaller than in solution, so that the ENDOR condition (8) can be fulfilled with much smaller H_2 fields.

As ENDOR signals are only some percent of the EPR intensity, ENDOR spectra often suffer from low signal-to-noise ratios. Unfortunately, it is not possible to increase the radical concentration to more than about 10^{-3} m. because at higher concentrations spin exchange diminishes the ENDOR enhancement[5].

ENDOR spectrometer

Fig. 4 shows the block diagram of the ENDOR spectrometer built in this laboratory[36].

The NMR transmitter is tunable in the range from 5 to 30 MHz, operating in the cw mode. The maximum rf output is 1 kW producing an NMR field at the sample of about 35 Oe (amplitude, rotating frame). The amplitude can be continuously adjusted and is electronically regulated within 5% over the whole frequency range.

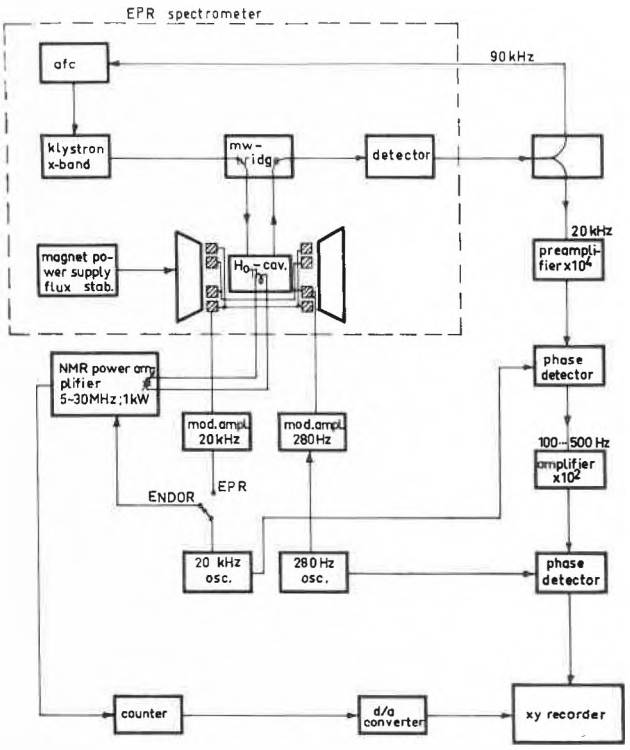

Figure 4. Block diagram of a cw high-power ENDOR spectrometer[36]

The tank circuit of the power tetrodes consists of a tunable vacuum capacitor and the NMR field producing two-turn loop which is placed within the H_{011} cylindrical cavity. The cavity is formed by a pile of 10 concentric rings, each of which is water cooled as is the rf loop. In order to reduce spurious signals the ENDOR signal is doubly coded by a low-frequency ZEEMAN modulation and a 20 kHz frequency modulation of the NMR oscillator. Due to the phase sensitive detection the ENDOR signals are recorded in a first derivative form. The overall stability of the ENDOR spectrometer is so high that ENDOR can even be performed on resolved hfs components without using a field-frequency-lock. CW-spectrometers with lower rf-field capability were described by MAKI *et al.*[1] and ALLENDOERFER *et al.*[28]. A pulsed spectrometer which is also commercially available (Varian) has been described in detail by HYDE[2,8].

Selected examples of ENDOR in isotropic solution

1. *Assignment of* ENDOR *lines*

For an assignment of hfs splitting constants to specific positions within the molecule it is important to know the number of contributing protons. In contrast to NMR and EPR this information is often obscured in ENDOR spectra. Fig. 5 shows as example the ENDOR spectrum of the radical tri-*t*-butyl-phenoxyl in mineral oil at room temperature. It is obvious, that the relative line

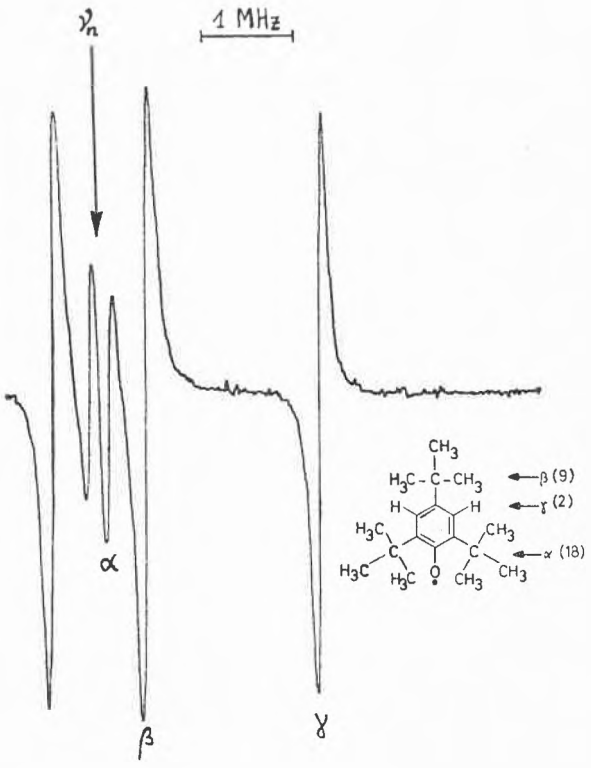

Figure 5. ENDOR spectrum of the tri-*t*-butyl-phenoxyl radical in mineral oil at room temperature. In parenthesis the number of equivalent protons is given

intensities do not at all reflect the number of contributing protons. One reason for this discrepancy is the dependence of the anisotropic dipole-dipole interaction—which is responsible for the nuclear relaxation rate W_n—on the unpaired spin density distribution throughout the radical. In principle it is possible to determine this interaction for each radical position by the formulae given by MCCONNELL and STRATHDEE[39], but a thorough investigation of this problem remains to be done. Preliminary attempts which only considered π contributions remained unsatisfactory[26]. For coupling constants which are comparable with the EPR line width parameter T_{2e}^{-1} the problem of independent saturation of different EPR-hfs-components has to be considered. Due to the overlap of the different EPR levels an independent saturation is no longer possible, so that the irradiating NMR field cannot enhance the EPR absorption. A quantitative analysis gives the observed relative ENDOR intensity[20,27]:

$$I_{obs} = I_{max} \frac{T_{2e}^2 \cdot A^2}{T_{2e}^2 \cdot A^2 + 0.063}, \qquad (9)$$

where I_{max} is given by the number of protons, and A is the hfs coupling in MHz.

Fortunately, there exist various possibilities to overcome the difficulty of assignment in ENDOR. The most convincing method is successive deuteration, as has been demonstrated for the triphenylphenoxyl radical[9]. Due to the large difference in gyromagnetic ratios of the proton and deuteron ($\gamma_P/\gamma_D \approx 6.5$) the ENDOR lines of the deuterons do not show up in the proton ENDOR spectrum. This is in contrast to EPR, where a simplification of the spectra only occurs if positions of low spin density are deuterated.

In case of different classes of protons exhibiting pronounced differences in the anisotropy of their hyperfine interactions, assignments can be facilitated by the different temperature dependences of the ENDOR line widths and intensities of these protons[9,23]. Such a difference exists, for instance, for ring and methyl protons. Whereas the anisotropy of ring protons amounts to about 50% of the isotropic coupling, the anisotropy of a rotating methyl group is only of the order of 10% of the isotropic coupling[40,41]. As a result, when cooling the sample and thereby increasing the viscosity of the solvent, the EPR and ENDOR lines of ring protons broaden at higher temperatures than the methyl proton lines because of the incomplete averaging of the anisotropic hyperfine interactions. This effect is clearly demonstrated in Fig. 6 for a pentaphenyl-cyclopentadienyl methyl derivative in isopentane, where with decreasing temperature the relative line intensities change drastically in favour of the methyl lines.

As was shown by FREED *et al.*[7], specific coherence effects can also be used to determine the number of protons contributing to an ENDOR line. As is well known from

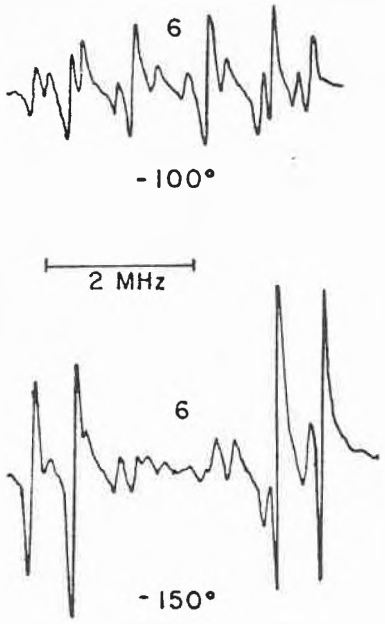

Figure 6. ENDOR spectra of 1,3,4-CH_3-pentaphenylcyclopentadienyl (for the numbering scheme see Fig. 8) in isopentane at different temperatures. The 4 most intense lines at -150 °C can be assigned to methyl protons (see text)

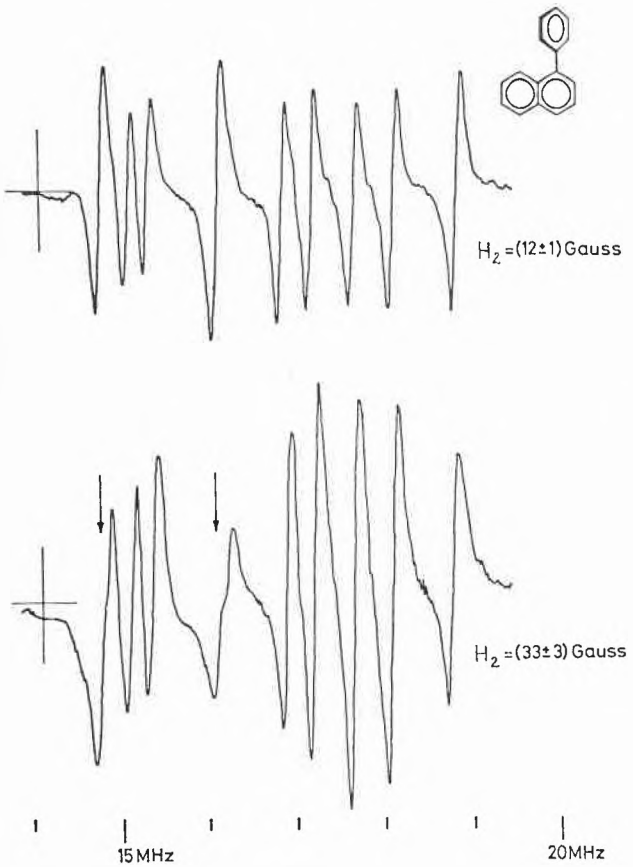

Figure 7. Part of the ENDOR spectrum of 1-phenyl-naphthalene anion radical in dimethoxyethane at two different NMR field strengths H_2 (the largest splitting is not shown). The lines exhibiting the coherence effect are marked with arrows

spin tickling experiments in NMR, in which both the irradiated and observed transitions have one energy level in common, coherence effects can influence the line shape either by a broadening or a splitting. In case of the 1-phenyl-naphthalene anion radical this effect has been used to determine the number of protons belonging to the particular ENDOR lines[34]. From theory it turns out, that under moderate microwave saturation only groups with $I > 1/2$ (i.e. more than one proton) can show a coherence effect at high NMR fields. Ion radicals require NMR fields as high as 35 gauss (amplitude, rotating frame) in order to produce detectable effects (see Fig. 7).

At any rate, it is advisable, to check the assignment of ENDOR lines by a subsequent computer simulation of the EPR spectrum. This means that ENDOR is no substitute for high resolution EPR. As ENDOR spectra often have to be recorded under conditions different from those for optimum EPR resolution, the ENDOR hfs constants may differ by some percent from the fitted EPR results.

2. ENDOR *studies of intramolecular conformational changes*

As is well known from EPR and NMR studies[42,52], dynamic intramolecular processes can produce relaxation that can show up in line width effects, provided the characteristic time constant of the dynamic interaction is comparable with the frequency separation between resonance lines in a spectral multiplet; several MHz for EPR spectra, or a few Hz in NMR. Temperature dependent coalescence of ENDOR lines has been observed for some aromatic radicals carrying mobile side chains as substituents[4, 11, 12, 15, 17]. This collapsing of lines was interpreted as being due to an increase in the jumping rate between different conformations, which represent different environments for the nuclear spins. Detailed studies of the ENDOR line width as function of temperature *above* the coalescence point resulted in reliable values for the activation energy and preexponential factors of the internal rotation of the side chain in vitamin K_1 and ubisemiquinone radical ions[17]. The quantitative analysis was performed in the fast jump region for a two-jump model in order to be able to make use of the relaxation theory developed by REDFIELD[43] and FREED[42]. The results obtained agree very well with the data from EPR line width effects. It is obvious that in case of low symmetry radicals the ENDOR technique can be a very powerful tool in analysing intramolecular processes.

3. ENDOR *study of the lifting of orbital degeneracy by methyl groups*[23, 25]

In general, the effect of a methyl substituent on the spin density distribution in a free radical is very small. However, as has been shown in EPR and NMR studies of the substituted benzene anion radicals[44, 45], the effect can be

significant if the orbital ground state of the parent radical is two-fold degenerate and methyl substitution, by lowering the symmetry, removes the degeneracy.

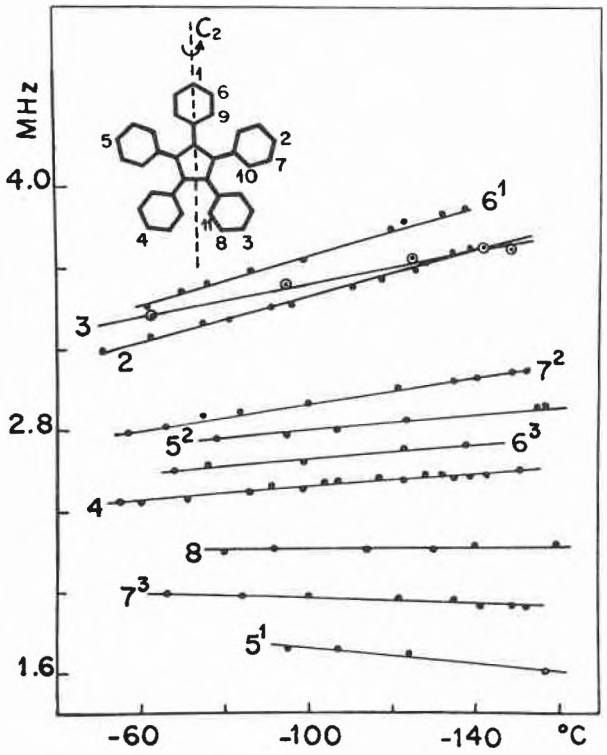

Figure 8. Methyl coupling constants of compound 2 through 8 in isopentane as a function of temperature

Compound (2): 1-CH_3-PPCPD; (3): 2,5-CH_3-; (4): 3,4-CH_3-; (5): 1,2,5-CH_3-; (6): 1,3,4-CH_3-; (7): 2,3,4,5-CH_3-; (8): 1,2,3,4,5-CH_3-

The observed position is indicated by a superscript

A HÜCKEL MO calculation for the pentaphenylcyclopentadienyl radical (PPCPD) and its penta-methyl derivative assuming D_5 symmetry shows that the unpaired electron occupies an orbital which is doubly degenerate. Incomplete *p*-methyl-substitution lowers the symmetry to C_2 thereby splitting the two lowest states by an amount ΔE. In the PPCPD derivatives ΔE is expected to be of the order of kT because of the strong electron delocalization. As a result the measured hfs constants will be a weighted average between the splittings in the symmetric and antisymmetric states. By means of the ENDOR technique it was feasible to analyze the hyperfine structure of the methyl substituted PPCPD radicals 2 through 8 (see Fig. 8) and study the temperature dependence of their methyl splitting constants. As result the symmetry of the ground states of the various PPCPD derivatives could be determined together with the corresponding energy gaps between the ground state and the thermally accessible excited doublet state. The results could be rationalized within the HMO scheme in terms of a simple electrostatic model of the CH_3 group.

4. ENDOR *studies of nuclei other than protons*

Considerable effort was invested to extend the ENDOR spectroscopy to nuclei other than protons. The first success was reported for ^{19}F in β-position, whereas no fluorine ENDOR lines could be observed so far for ^{19}F in α-position, i.e. fluorine directly bonded to the π-system[13]. A possible explanation for this observation is given by the pronounced difference in the anisotropy of the fluorine hyperfine tensors in α- and β-position. For α-fluorine the traceless part of the hfs tensor is much larger than for β-fluorines[46]. Therefore it may be extremely difficult to saturate the NMR transitions in the slow motion temperature region ($\omega_e \tau_R \gg 1$), which means that condition (5) cannot be fulfilled. In addition line broadening will occur because there is no complete averaging of the traceless part of the hfs tensor. We expect α-fluorine ENDOR to be possible at elevated temperatures where $\omega_e \tau_R \ll 1$. In this region, however, W_e will normally exceed W_n considerably so that according to condition (6) only small ENDOR enhancements will be observed.

Similar problems are expected for ENDOR work on ^{13}C nuclei because of the large anisotropic hfs tensor. Recently, however, we succeeded in observing ^{13}C-ENDOR of isotopically enriched benzophenone anion radicals (Fig. 9)[37]. In order to avoid interference of the

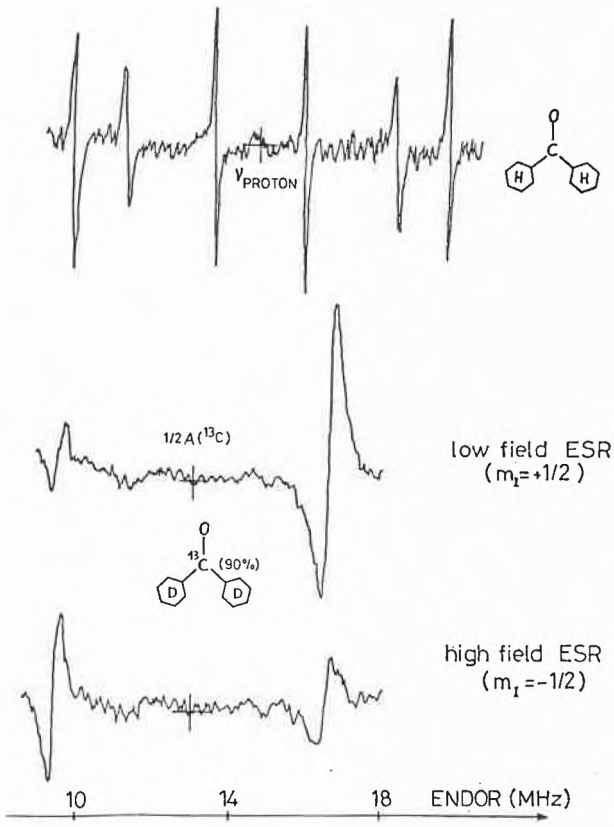

Figure 9. Proton and ^{13}C ENDOR spectra of benzophenone anion radical in dimethoxyethane at 210 °K and 270 °K, respectively. The m_I dependence of the relative ^{13}C ENDOR line intensities can be attributed to cross relaxation (see text)

weak ^{13}C lines with the large proton lines, the sample was perdeuterated. A detailed study of the various relaxation mechanisms, contributing to the ^{13}C-ENDOR enhancement is in progress.

For nuclei with a gyromagnetic ratio considerably smaller than that of protons, discouraging large NMR fields are to be expected according to eq. (8). With nitroxide radicals as an example, LENIART *et al.*[19] have shown that by means of the rf enhancement factor, which increases the effective NMR field at the nucleus, ENDOR-in-solution for such nuclei will nevertheless be possible, provided the isotropic hfs coupling constant is sufficiently large. From a simple physical picture[47] the effective NMR field can be deduced to be

$$H_2^{\text{eff}} = H_2\left(1 - m_s \cdot \frac{A'}{H_0} \cdot \frac{\gamma_e}{\gamma_p} \cdot \frac{\gamma_p}{\gamma_I}\right), \qquad (10)$$

where A' is the isotropic hfs constant in gauss.

For the radicals studied A' was in the order of 15 gauss, resulting in an enhancement factor of 21.

By use of this formula, we can estimate that for *any* nucleus ENDOR-in-solution will be possible if A' is at least in the order of 10 gauss. For this estimate we have required, that the rf induced transition rates should be the same as for protons, equal NMR line widths provided.

The ENDOR spectra of ^{14}N and ^{13}C nuclei have one feature in common: The two ENDOR lines are of different intensity, and the intensity ratio depends on the m_I-value of the saturated EPR transition. As can be seen from Fig. 3, this can be explained by considering cross relaxations with the rates W_{x_1} and W_{x_2}. Generally these rates are different. In the limiting case of fast tumbling ($\omega_e \tau_R < 1$) and predominant anisotropic electron nuclear dipole dipole interaction one obtaines $W_{x_2} = 4\,W_n$ and $W_{x_1} = \frac{2}{3}\,W_n$[19]. Obviously there is a difference in the effectiveness of these additional relaxation paths when saturating different EPR transitions. By increasing the viscosity of the solvent, and thereby τ_R, cross relaxation can be switched off[35], resulting in nearly equally intense ENDOR lines.

5. ENDOR *in liquid crystals*

When performing spectroscopy in isotropic solvents information is lost because the measured interactions represent only the traces of the tensors in the corresponding Spin-Hamiltonian, whereas anisotropic contributions are averaged to zero by the Brownian motion of the molecules. Only in favourable cases, the width of the hyperfine lines can be used to extract some information about anisotropic interactions[48].

However, by using a liquid crystal as solvent, the molecular motion of the solute molecules can be restricted in such a way that they become partially aligned. In magnetic resonance experiments liquid crystals with a nematic mesophase are especially suitable, because an alignment can be achieved by magnetic fields of some kilogauss[13].

As a consequence the positions of the hyperfine lines now depend additionally on the magnitude of the anisotropic interactions and on the degree of alignment[50].

The magnitude of the shift of the hfs lines between isotropic and nematic phases is given by[50]:

$$\Delta a = O_{33} A'_{33} + \frac{1}{3}(O_{11} - O_{22})(A'_{11} - A'_{22}) \qquad (11)$$

where the $O_{ii} = \frac{1}{2}(3\overline{l_i\, l_i} - 1)$ and the A'_{ii} are the elements of the traceless ordering and hyperfine tensors, respectively (l_i is the direction cosine between the molecular axes i and the magnetic field direction).

If at least one of these tensors is axially symmetric, eq. (11) reduces to

$$\Delta a = O_{33} \cdot A'_{33}. \qquad (12)$$

From the measured shift one can therefore deduce the ordering parameter when the hyperfine tensor component is known or vice versa. From the sign of the shift it is furthermore possible to determine the sign of the isotropic hyperfine coupling constant and thereby the sign of the π spin density[50].

With EPR these advantages of liquid crystals have been demonstrated already in some detail[50,51]. When applying these ideas to ENDOR, the main difficulty arises from finding a suitable liquid crystal. Because of the complex relaxation mechanisms which are responsible for proton ENDOR enhancements, one is restricted to solvents of rather high viscosity[3]. Unfortunately, common liquid crystals like *p*-azoxyanisole exhibit nematic properties at rather elevated temperatures where their viscosity is quite small. Very recently, however, room-temperature liquid crystals of high viscosity became available. Good ENDOR enhancements could be achieved in the «Phase IV» liquid crystal (Merck, Darmstadt)[33].

We have performed ENDOR in liquid crystal experiments on the radicals: perinaphthenyl (PNT), tri-*t*-butylphenoxyl (TBP)[33], and some nitroxide radicals[35]. PNT was chosen to probe the degree of order of the new solvent "Phase IV". The TBP radical was studied in the liquid crystal because the determination of the signs of the splitting constants was necessary to test the predictions of different MO theories.

The nitroxide radicals were investigated to determine the quadrupole coupling of a molecule in solution[35]. For molecules in isotropic solutions quadrupole interactions cannot produce stationary lineshifts, as the interaction is represented by a traceless second rank tensor, the contribution of which is averaged to zero by rapid tumbling.

Even if the solute molecules are partially aligned by a nematic liquid crystal in a magnetic field, the quadrupole interaction cannot influence the positions of the

EPR lines, because the coupling shifts all levels connected by EPR transitions equally[50].

The appropriate Spin-Hamiltonian for a doublet radical in the nematic phase of a liquid crystal in a magnetic field has the form[35]:

$$\bar{\mathcal{H}} = \bar{\mathcal{H}}_{ZE} + \bar{\mathcal{H}}_{HFS} + \bar{\mathcal{H}}_{ZN} + \bar{\mathcal{H}}_{Q}$$

with

$$\bar{\mathcal{H}}_{ZE} = g\beta \boldsymbol{H}_0 \boldsymbol{S}_Z + \left\{g'_{33} O_{33} + \frac{1}{3}(g'_{11} - g'_{22})(O_{11} - O_{22})\right\} \beta \boldsymbol{H}_0 \boldsymbol{S}_Z, \quad (13)$$

$$\bar{\mathcal{H}}_{HFS} = A \cdot \boldsymbol{I}\boldsymbol{S} + \left\{A'_{33} O_{33} + \frac{1}{3}(A'_{11} - A'_{22})(O_{11} - O_{22})\right\} \times \left\{\boldsymbol{I}_Z \boldsymbol{S}_Z - \frac{1}{4}(\boldsymbol{I}_+ \boldsymbol{S}_- + \boldsymbol{I}_- \boldsymbol{S}_+)\right\} \quad (14)$$

$$\bar{\mathcal{H}}_{ZN} = -g_I \beta_I \boldsymbol{H}_0 \boldsymbol{I}_Z, \quad (15)$$

$$\bar{\mathcal{H}}_{Q} = Q' \left\{O_{33} + \frac{1}{3}\eta (O_{11} - O_{22})\right\} \times \left\{\boldsymbol{I}_Z^2 - \frac{1}{3} I(I+1)\right\}, \quad (16)$$

where

$$Q' = \frac{3e^2 q'_{33} Q}{4I(2I-1)}, \quad \eta = \frac{q'_{11} - q'_{22}}{q'_{33}}.$$

The various tensor components refer to the corresponding molecule fixed principal axes. The primed components refer to the traceless parts of the various interactions. As we treat only the interaction with the nitrogen nucleus, the summation over the other nuclei is omitted. Setting

$$A'_{33} O_{33} + \frac{1}{3}(A'_{11} - A'_{22})(O_{11} - O_{22}) = B, \quad (17)$$

$$Q' \left\{O_{33} + \frac{1}{3}\eta (O_{11} - O_{22})\right\} = \overline{Q'} \quad (18)$$

and

$$\frac{\left(A - \frac{1}{2}B\right)^2}{2g\beta H_0} = C,$$

the energy eigenvalues up to second order are:

$$E_{m_s m_I} = \tilde{g}\beta H_0 m_s - \tilde{g}_I \beta_I H_0 m_I + (A + B) m_s m_I - C m_s m_I^2 + \overline{Q'} m_I^2, \quad (19)$$

where

$$\tilde{g} = g\left\{1 + \frac{CI(I+1)}{g\beta H_0}\right\}, \quad \tilde{g}_I = g_I\left\{1 + \frac{C}{2g_I \beta_I H_0}\right\}$$

[In (19), terms not depending on m_s or m_I have been omitted as they do not effect the EPR and ENDOR spectra.]

By saturating alternatively the three different EPR hfs components ($m_I = -1, 0, +1$), one obtains the following ENDOR frequencies:

$$h\nu_{ENDOR}(m_I = -1) = \frac{1}{2}(A + B) \pm (\tilde{g}_I \beta_I H_0 + \overline{Q'}) + \frac{C}{2}, \quad (2$$

$$h\nu_{ENDOR}(m_I = +1) = \frac{1}{2}(A + B) \pm (\tilde{g}_I \beta_I H_0 - \overline{Q'}) - \frac{C}{2}, \quad (2$$

$$h\nu_{ENDOR}(m_I = 0) = \begin{cases} \frac{1}{2}(A + B) + \tilde{g}_I \beta_I H_0 \pm \left(\overline{Q'} + \frac{C}{2}\right) \\ \frac{1}{2}(A + B) - \tilde{g}_I \beta_I H_0 \pm \left(\overline{Q'} - \frac{C}{2}\right). \end{cases} \quad (2$$

As can be seen from (22) the EPR hfs component $m_I = 0$ can be desaturated by *four* different NMR transitions, whereas for the other two hfs components this is only possible by *two* NMR transitions. The two pairs of ENDOR lines for $m_I = -1$ and $m_I = +1$ are separated by $2\tilde{g}_I \beta_I H_0 + 2\overline{Q'}$ and $2\tilde{g}_I \beta_I H_0 - 2\overline{Q'}$, respectively. Thus by measuring the difference of these separations one directly obtains $4\overline{Q'}$. From the centers of gravity of these two pairs of ENDOR lines one can furthermore deduce the magnitude of the second order shift C.

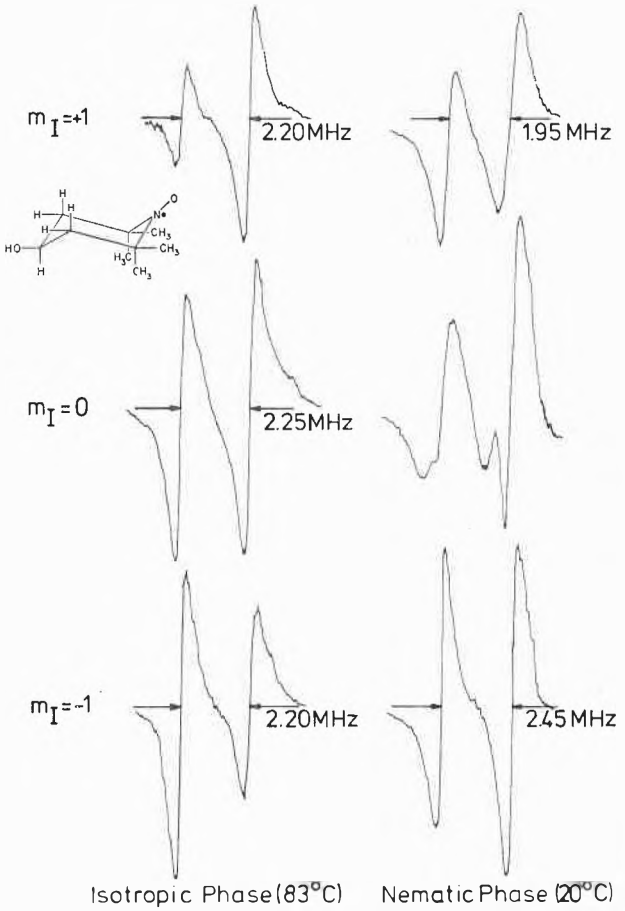

Figure 10. ^{14}N ENDOR spectra of tanol in the isotropic and nematic phase of a room-temperature liquid crystal. For the evaluation of the quadrupole coupling see text

Fig. 10 shows the nitrogen ENDOR spectra of tanol in the isotropic and nematic phases. The influence of second order and cross relaxation effects on the spectra are discussed elsewhere[35]. The interpretation of the observed quadrupole shift requires axial symmetry of either the ordering or quadrupole tensors. For the nitroxide radicals studied the asymmetry part in (18) turned out to be so small that a value of

$$e^2 q'_{33}\, Q/h = -2.5 \text{ MHz}$$

could be extracted (O_{33} can be easily obtained from EPR measurements[35]).

Because the sign of the ^{14}N hfs splitting constant can be safely predicted, these experiments yield even the sign of the quadrupole coupling. This result could be rationalized by a TOWNES-DAILEY population analysis of the nitrogen bonds. The theory predicts that the main contribution to the observed splitting comes from the unpaired π-electron.

Acknowledgment

It is a pleasure to acknowledge the support from our collaborators R. BIEHL, M. PLATO, and H. HAUSTEIN. We want to thank the Deutsche Forschungsgemeinschaft for financial assistance.

Appendix

Literature survey of ENDOR *in liquid solution work*

I. Experimental techniques (2, 8, 10, 22, 28, 36)
II. Theory (3, 5, 7, 13, 14)
III. Proton ENDOR of neutral radicals
  1. Triphenylmethyl and its derivatives (2, 4, 9, 10, 12, 13, 15)
  2. Diphenylmethane derivatives (11)
  3. Perinaphthenyl (33,34)
  4. Pentaphenylcyclopentadienyl and its methyl derivatives (23, 25)
  5. Phenoxyl radicals and their derivatives (1, 2, 6, 16, 20, 28, 32, 33)
  6. Nitroxide radicals (8, 19, 27, 35)
  7. Phenylsubstituted imidazyl and pyrryl radicals (30)
  8. Flavin radicals (8)
IV. Proton ENDOR of ion radicals
  1. Pure aromatic hydrocarbon radicals (2, 18, 26, 29, 31, 34)
  2. Semiquinone radicals (2, 17, 21, 22)
V. Non-proton ENDOR
  1. ^{19}F in hexakis (trifluoromethyl)benzene anion (13)
  2. ^{14}N in nitroxide radicals (19, 35)
  3. ^{13}C in benzophenone anion (37)

Literature

1 J. S. HYDE and A. H. MAKI, *J. Chem. Physics 40* (1964) 3117.
2 J. S. HYDE, *J. Chem. Physics 43* (1965) 1806
3 J. H. FREED, *J. Chem. Physics 43* (1965) 2313.
4 J. S. HYDE, R. BRESLOW, and CH. DEBOER, *J. Amer. Chem. Soc. 88* (1966) 4763.
5 J. H. FREED, *J. Physic. Chem. 71* (1967) 38.
6 J. S. HYDE, *J. Physic. Chem. 71* (1967) 68.
7 J. H. FREED, D. S. LENIART, and J. S. HYDE, *J. Chem. Physics 47* (1967) 2762.
8 J. S. HYDE, in A. EHRENBERG, B. G. MALMSTRÖM, and T. VÄNNGÅRD (Eds.), *Magnetic Resonance in Biological Systems*, Pergamon Press, Oxford 1967, p. 63.
9 J. S. HYDE, G. R. RIST, and L. E. G. ERIKSSON, *J. Physic. Chem. 72* (1968) 4269.
10 A. H. MAKI, R. D. ALLENDOERFER, J. C. DANNER, and R. T. KEYS, *J. Amer. Chem. Soc. 90* (1968) 4225.
11 C. STEELINK, J. D. FITZPATRICK, L. D. KISPERT, and J. S. HYDE, *J. Amer. Chem. Soc. 90* (1968) 4354.
12 L. D. KISPERT, J. S. HYDE, CH. DEBOER, D. LAFOLLETTE, and R. BRESLOW, *J. Physic. Chem. 72* (1968) 4276.
13 R. D. ALLENDOERFER and A. H. MAKI, *J. Amer. Chem. Soc. 91* (1969) 1088)
14 J. H. FREED, *J. Chem. Physics 50* (1969) 2271.
15 H. D. BRAUER, H. STIEGER, J. S. HYDE, L. D. KISPERT, and G. R. LUCKHURST, *Mol. Physics 17* (1969) 457.
16 R. F. ADAMS and N. M. ATHERTON, *Mol. Physics 17* (1969) 673.
17 M. R. DAS, H. D. CONNOR, D. S. LENIART, and J. H. FREED, *J. Amer. Chem. Soc. 92* (1970) 2258.
18 A. LAGENDIJK, N. F. M. TROMP, M. GLASBEEK, and J. D. W. VAN VOORST, *Chem. Physic. Lett. 6* (1970) 152.
19 D. S. LENIART, J. C. VEDRINE, and J. S. HYDE, *Chem. Physic. Lett. 6* (1970) 637.
20 R. D. ALLENDOERFER and A. H. MAKI, *J. Magn. Res. 3* (1970) 396.
21 R. D. ALLENDOERFER and R. J. PAPEZ, *J. Amer. Chem. Soc. 92* (1970) 6971.
22 R. J. COOK and D. G. MOSS, *Proceedings of the XVIth Congress Ampère, Bukarest 1970*, p. 1109.
23 K. MÖBIUS, H. VAN WILLIGEN, and A. H. MAKI, *Proceedings of the XVIth Congress Ampère, Bukarest 1970*, p. 1114.
24 N. M. ATHERTON, A. J. BLACKHURST, and I. P. COOK, *Chem. Physic. Lett. 8* (1971) 187.
25 K. MÖBIUS, H. VAN WILLIGEN, and A. H. MAKI, *Mol. Physics 20* (1971) 289.
26 R. BIEHL, K. P. DINSE, and K. MÖBIUS, *Chem. Physic. Lett. 10* (1971) 605.
27 R. D. ALLENDOERFER and J. H. ENGELMANN, *Mol. Physics 20* (1971) 569.
28 R. D. ALLENDOERFER and D. J. EUSTACE, *J. Physic. Chem. 75* (1971) 2765.
29 R. D. ALLENDOERFER and R. CHANG, *J. Magn. Res. 5* (1971) 273.
30 R. D. ALLENDOERFER and A. S. POLLOCK, *Mol. Physics 22* (1971) 661.
31 A. L. SHAIN, *Mol. Physics 22* (1971) 733.
32 N. M. ATHERTON, A. J. BLACKHURST, and I. P. COOK, *Trans. Farad. Soc. 67* (1971) 2510.
33 K. P. DINSE, R. BIEHL, K. MÖBIUS, and H. HAUSTEIN, *Chem. Physic. Lett. 12* (1971) 399.
34 K. P. DINSE, R. BIEHL, K. MÖBIUS, and M. PLATO, *J. Magn. Res. 6* (1972) 444.
35 K. P. DINSE, K. MÖBIUS, M. PLATO, R. BIEHL, and H. HAUSTEIN, *Chem. Physic. Lett.*, in press.
36 K. P. DINSE, *Z. Naturforsch.*, to be published.
37 K. P. DINSE, K. MÖBIUS, R. BIEHL, and M. PLATO, *Proceedings of the XVIIth Congress Ampère, Turku 1972*, to be published
38 G. FEHER, *Physic. Rev. 103* (1956) 834.
39 H. M. MCCONNELL and J. STRATHDEE, *Mol. Physics 2* (1959) 129.
40 H. M. MCCONNELL, C. HELLER, T. COLE, and R. W. FESSENDEN, *J. Amer. Chem. Soc. 82* (1960) 766.
41 J. R. MORTON and A. HORSFIELD, *J. Chem. Physics 35* (1961) 1142.

42 J.H.Freed and G.K.Fraenkel, *J. Chem. Physics 39* (1963) 326.
43 A.G.Redfield in *Advances in Magnetic Resonance I* (J.S. Waugh, Ed.), Academic Press, New York 1965.
44 J.R.Bolton and A.Carrington, *Mol. Physics 4* (1961) 497.
45 E.deBoer and J.P.Colpa, *J. Physic. Chem. 71* (1967) 21.
46 M.Iwasaki, S.Noda, and K.Toriyama, *Mol. Physics 18* (1970) 201.
47 S.Geschwind, in Hyperfine Interactions (A.J.Freeman and R.B.Frankel, Ed.), Academic Press, New York 1967.
48 A.Hudson and G.R.Luckhurst, *Chem. Rev. 69* (1969) 161.
49 G.W.Gray, *Molecular structure and the properties of liquid crystals*, Academic Press, New York 1962.
50 H.R.Falle and G.R.Luckhurst, *J. Magn. Res. 3* (1970) 161.
51 H.Haustein, K.Möbius, and K.P.Dinse, *Z. Naturforsch. 24a* (1969) 1764, 1768; *26a* (1971) 1230.
52 A.Carrington and A.D.McLachlan, *Introduction to Magnetic Resonance*, Harper & Row, New York 1967.
53 R.Biehl, unpublished results.